Title	Acceleration of deposition of AB1-40 peptide on ultrasonically formed AB1-42 nucleus studied by wireless quartz-crystal-microbalance biosensor
Author(s)	Ogi, Hirotsugu; Fukushima, Masahiko; Uesugi, Kentaro et al.
Citation	Biosensors and Bioelectronics. 2012, 40(1), p. 200-205
Version Type	AM
URL	https://hdl.handle.net/11094/84196
rights	© 2012 Elsevier B.V. This manuscript version is made available under the Creative Commons Attribution-NonCommercial-NoDerivatives 4.0 International License.
Note	

Acceleration of deposition of Aβ_{1-40} peptide on ultrasonically formed Aβ_{1-42} nucleus studied by wireless quartz-crystal-microbalance biosensor

Hirotsugu Ogi[a,*], Masahiko Fukushima[a],

Kentaro Uesugi[a], Hisashi Yagi[b], Yuji Goto[b], Masahiko Hirao[a]

[a] *Graduate School of Engineering Science, Osaka University*

Machikaneyama 1-3, Toyonaka, Osaka 560-8531, Japan

[b] *Institute for Protein Research, Osaka University*

Yamadaoka 3-2, Suita, Osaka 565-0871, Japan

Abstract

High-frequency ($\sim$55 MHz) wireless quartz-crystal microbalance biosensor was used for studying heterogeneous deposition behavior of Aβ_{1-40} peptide on Aβ_{1-42} nuclei, which were grown under the stirring agitation and 200-kHz ultrasonication at pH 2.2, 4.6, and 7.4. The deposition reaction was monitored over 40 h, and the deposition rate was deduced. Among the agitation nuclei, the maximum deposition rate was observed on the nucleus grown at pH 4.6. However, ultrasonication nucleus grown at pH 7.4 produced much larger deposition rate, despite the same β-sheet concentration. This result indicates that local structural modulation is caused in the nucleus by ultrasonication, which adsorbs the Aβ peptide more actively than other nuclei. The resultant deposits clearly show oligomeric structure.

---

1 Introduction

It is widely recognized that the pathogenesis of Alzheimer's disease (AD) is closely related with aggregations of amyloid β (Aβ) peptides (Lambert *et al.* (1998); LaFerla *et al.* (2007)). There are two principal Aβ peptides, Aβ_{1-40} and Aβ_{1-42}, consisting of 40 and 42 amino acids, respectively. They form various aggregations in neurons, and some of them are significantly neurotoxic, eventually resulting in AD. Therefore, understanding of the aggregation mechanism of the Aβ peptides is important for identifying target aggregates and developing drugs to decompose them. The aggregation processes of amyloidosis peptides were studied in bulk solutions in the past (Jarrett *et al.* (1993); Wood *et al.* (1996); Bitan *et al.* (2003); Benseny-Cases *et al.* (2007); Isaacs *et al.* (2010); Ladiwala *et al.* (2010)). However, polymerization of the peptides in a bulk solution fails to avoid interactions among aggregates and makes it difficult to quantify the most important interaction between the nuclei and surrounding monomer peptides.

Recently, we have succeeded in a long-time monitoring of deposition of Aβ peptides on nuclei immobilized on the sensor surface using the homebuilt wireless quartz-crystal microbalance (QCM) biosensor (Ogi *et al.* (2009a)) and studied deposition behaviors of Aβ_{1-40} and Aβ_{1-42} on their nuclei (Ogi *et al.* (2011)): The deposited structures were significantly different from those formed in the bulk solution by agitation, indicating the importance of the study of interaction between nuclei and monomer, not among aggregates. Also, a high deposition rate was observed in the case of the heterogeneous

2

deposition, where $A\beta_{1-40}$ peptide markedly accumulated on $A\beta_{1-42}$ nucleus, resulting in oligomeric structures (Ogi *et al.* (2011)). This observation can be an important model for AD because of three reasons: (i) $A\beta_{1-42}$ is more hydrophobic (Jarrett *et al.* (1993)) and can self-associate to form nuclei immediately just after its production from the amyloid precursor protein (APP) by the cleaving enzymes (β- and γ-secretases) (LaFerla *et al.* (2007)), (ii) most of the produced peptides is $A\beta_{1-40}$ (Suzuki *et al.* (1994); Iwatsubo *et al.* (1994); Gravina *et al.* (1995)), which can be the major material to form the aggregates, and (iii) oligomers are more neurotoxic than fibrils (Lambert *et al.* (1998); Klein *et al.* (2001); Mastrangelo *et al.* (2006)).

Not only the structural evaluation, but also searching such a nucleus that can adsorb $A\beta$ monomers with a high rate is an important issue for the drug development process, because it will contribute to fabricate neurotoxic aggregates in a short time. For this purpose, here we focus on ultrasonication for preparation of nuclei: Goto and coworkers displayed acceleration of amyloid nucleation and fibril formation from monomeric β_2-microglobulin, an amyloidosis peptide, by ultrasonication (Ohhashi *et al.* (2005); Chatani *et al.* (2009); So *et al.* (2011)). Their studies suggest that ultrasonication lowers the free-energy barrier for the transformation of monomers into protofibrils (Chatani *et al.* (2009)) and induces nucleation of fibrils within a few hours, which would take a much longer time without ultrasonic irradiation. They expect that this will be a common phenomenon among various amyloidosis peptides, including $A\beta$ (So *et al.* (2011)).

Thus, in this study, we systematically investigate the deposition rate in the heterogeneous deposition of $A\beta_{1-40}$ peptide on immobilized $A\beta_{1-42}$ nuclei, which are prepared with and without ultrasonic irradiation under pH 2.2,

4.6, and 7.4. The antenna-improved multichannel wireless QCM system is developed to monitor a long-time deposition reaction, whose capability is first confirmed by monitoring the binding reaction between β-secretase and APP fragment. Then, the deposition reaction of Aβ_{1-40} peptide is monitored at a neutral pH. We emphasize that only a QCM biosensor achieves these measurements, because of its large dynamic range; it keeps high sensitivity to the accumulation of monomers on large aggregates, whereas the surface-plasmon-resonance biosensor, for example, cannot detect adsorbed monomers on large aggregates when they interact outside the sensitive (evanescent) region.

The β-sheet concentration in nuclei is evaluated by the thioflavin T (ThT) fluorescence, and structures of nuclei and deposits are evaluated by an atomic-force microscopy (AFM). The results in the present study clearly show enlarged deposition rate on the nucleus prepared with ultrasonication.

2   Measurements

2.1   Materials and instruments

For the β-secretase, we obtained β-site APP cleaving enzyme 1 (BACE1) from Sigma (S4195). The Swedish-mutation APP fragment (H-Ser-Glu-Val-Asn-Leu-Asp-Ala-Glu-Phe-Arg-OH) was obtained from BACHEM (H-4834) as the target material of the β-secretase. Human IgG (hIgG) was from Athens Research and Technology, Inc. (16-16-090707). Staphylococcus aureus protein A (SPA) was from Zymed Laboratories, Inc. (10-1100). Bovine serum albumin (BSA) were from Sigma-Aldrich Japan (9048-46-8) . Lyophilized Aβ peptides were from the Peptide Institute (4307-v for Aβ40 and 4349-v for Aβ42). The

10-carboxy-1-decanethiol (10-CDT) and 1-ethyl-3-(3-dimethylaminopropyl)carbodiimide, hydrochloride (EDC) were from Dojindo (C385 and W001, respectively). Phosphate buffered saline (PBS) powder, acetic-acid sodium-acetate buffer solution (AAB), Glycine-HCl buffer (GHB) solution, dimethyl sulfoxide (DMSO), and ThT were from Wako Pure Chemical Industries, Ltd.

The high-power gated amplifier and superheterodyne spectrometer were produced by RITEC Inc. (RAM 1-200 MHz). The high-power (200 W) ultrasonic irradiation system was by KAIJO Corporation (model 4021). The AFM system was by Shimadzu Co. Ltd. (SPMA 9600). ThT fluorescence was measured by a fluorescence spectrometer by JASCO Corporation (FP-6200).

2.2 Preparation of $A\beta_{1-42}$ nuclei and $A\beta_{1-40}$ flowing solution

The lyophilized $A\beta_{1-42}$ peptide was dissolved in DMSO and diluted to a final concentration of 12 μM by PBS, AAB, or GHB solutions for adjusting pH values at 7.4, 4.6, or 2.2, respectively. Two methods were used for growing nuclei. One is the agitation by stirring the $A\beta_{1-42}$ solutions at a rotation speed of 1000 rpm for 48 h. The other is ultrasonication at 200 kHz with 200 W power: A microtube (material: polypropylene, capacity: 1.5 ml) containing a 500 μl $A\beta_{1-42}$ solution was located in a water tank (0 °C) so as to make the solution level lower than the water level. A flat ultrasonic transducer with a diameter of 70 mm was located below the microtube. The distance between the ultrasonic transducer and the bottom of the microtube was 30 mm. A 200-kHz longitudinal continuous wave was upward generated from the transducer, which entered the inside of microtube to cause ultrasonication to the peptide solution. We repeated the ultrasonication cycle (1-min ultrasonic irradiation

and 9-min break time) for totally 4 h.

We prepared the 12 μM Aβ_{1-40} monomer solution by dissolving the lyophilized Aβ_{1-40} in DMSO and diluting it with PBS.

2.3   Wireless QCM measurement

Details of our homebuilt wireless-QCM system are given in the supplemental material (Figure S1). Three or four sensor chips were used to obtain multiple reaction data with a single flow measurement. Quartz crystals were immersed in a piranha solution (98% H$_2$SO$_4$: 33% H$_2$O$_2$=7:3) for 10 min, and after rinsing with ultrapure water several times, they were immersed in a 10 μM 10-CDT/ethanol solution for 12 h. The sensor surfaces were activated using a 100 mM EDC solution for 1 h at 37 °C. After rinsing with the buffer solution, the crystals were immersed in the nucleus solutions for 5 h at 4 °C. The crystals were then set in the sensor cell, and the Aβ_{1-40} solution was flowed with the flow rate of 500 μL/min.

2.4   Binding reaction between β-secretase and APP

Because standard specific binding reactions between biomolecules are completed within 1 h, they cannot be used for evaluating the long-time-monitoring capability. We then focus on early stage of a protease reaction, which takes much longer time ($>\sim$10 h) (O'Meara and Munro (1984)). For this purpose, we monitored the binding reaction of β-secretase onto the APP fragment over 30 h. We immobilized the APP fragment (0.1 mg/ml APP fragment in PBS), which includes the β-secretase cleavage site near aspartic acid (Asp) (Yan

6

et al. (1999)), on the sensor surfaces using 10-CDT and EDC as described above. The sensor surfaces were then blocked by 50 mM glycine. We also prepared reference sensor chips, on which BSA and glycine were immobilized for checking negative binding behavior. We flowed 5 μg/ml BACE1/PBS solution on them. Furthermore, we prepared SPA immobilized sensor chip with BSA blocking for comparing the specific binding reaction between SPA and hIgG with that between β-secretase and APP fragment.

2.5   ThT fluorescence analysis

The ThT fluorescence assay is widely adopted for evaluating formation of amyloid fibrils, including protofibrils and their extensions (Naiki *et al.* (1990); Ban *et al.* (2004)). It uses enhanced light emission from ThT molecules that specifically binds to the β-sheet structures (Naiki *et al.* (1989)). We prepared a stock solution for the ThT analysis by dissolving ThT in a glycine/sodium-hydroxide buffer solution (pH 8.5) with a final concentration of 5 μM. A 100 μl sample solution was mixed with a 1-ml stock solution, and the mixture solution was poured into a quartz-glass cell for the fluorospectrophotometer. The fluorescence level was measured at 490 nm for the excitation at 450 nm. We performed the ThT fluorescence analysis for the nucleus solutions containing $A\beta_{1-42}$ and for the flowing solution of $A\beta_{1-40}$ peptide.

2.6   AFM observation

Morphologies on the sensor surfaces before and after the deposition reaction were measured using a tapping-mode AFM with a silicon cantilever, showing

the resonance frequency near at 300 kHz.

3   Results

3.1   Binding between β-secretase and APP

Figure 1 compares frequency changes observed during the various binding reactions. (Note that logarithmic scale is used in the horizontal axis.) In the case of the specific binding reaction between hIgG and the immobilized SPA, the frequency change was saturated by nearly 30 min, whereas the frequency continued to decrease over 30 h in the case of the binding reaction of β-secretase on the APP fragment. Frequency changes of BSA and glycine sensor chips were, however, significantly smaller.

[Insert Figure 1 here.]

3.2   ThT level of nuclei

Figures 2(a) and 2(b) show changes in the ThT fluorescence level at 490 nm and the fluorescence spectrum during growth of $A\beta_{1-42}$ nuclei, respectively. Agitation by stirring the peptide solution raised the ThT level gradually, indicating formation of nucleus including the β-sheet structures. The ThT level showed the maximum value at pH 4.6, while it remained low value at pH 2.2 (Figure 2(c)). On the other hand, ultrasonication rapidly increased the ThT level at the neutral pH: It raised the ThT level for 4 h up to the same value as the maximum level achieved by the agitation. The ThT level after ultrasoni-

8

cation for 4 h exhibited strong pH dependence (Figure 2(c)), which remained low at pH 4.6 and 2.2. The ThT level of the flowing solution of $A\beta_{1-40}$ was also measured every after the deposition reaction for 50 h, but it remained the baseline level.

[Insert Figure 2 here.]

3.3 Heterogeneous deposition rate

Figures 3(a) and 3(b) show the frequency changes during the heterogeneous deposition of $A\beta_{1-40}$ peptide on the various $A\beta_{1-42}$ nuclei. For the nuclei formed by the agitation, the amount of frequency change was the largest on the nucleus grown at pH 4.6. However, the deposition reaction proceeds more significantly on the nucleus formed by ultrasonication at pH 7.4.

In Figure 4, we calculated the average deposition rate from the frequency change at 50 h using the Sauerbrey equation (Sauerbrey (1959)), which corresponds to the number of $A\beta_{1-40}$ monomer adsorbed on the area of 1 nm^2 in 1 year. Clearly, the deposition rate shows the maximum value for the deposition on the nucleus formed by ultrasonication at the neutral pH. (We have shown that the Sauerbrey equation can be utilized for evaluating adsorbed mass quantitatively with the higher-frequency QCM, because the mass loading effect is enhanced compared with viscosity and water-mass-loading effects at high frequencies (Ogi *et al.* (2009b)).)

[Insert Figure 3 here.]

[Insert Figure 4 here.]

3.4 AFM observation

Using AFM, we observed apparent structures of the nuclei formed by agitation and ultrasonication at different pH and found no considerable differences among them. They showed nearly spherical nuclei with 0.1-1 μm in diameters. However, the deposited structures on them were different as shown in Figure 5. (We cannot identify a characteristic deposited structure on the nuclei grown at pH 2.2.) The deposited structure on the nucleus by the agitation at pH 7.4 showed coexistence of the amyloid fibril and spherical aggregate (Figure 5(a)), but that at pH 4.6 consisted only of spherical aggregate (Figure 5(b)). The deposited structure on the nucleus formed by ultrasonication also consisted of spherical aggregate, and its density was much larger on the nucleus grown at pH 7.4 (Figure 5(c)) than at pH 4.6 (Figure 5(d)).

[Insert Figure 5 here.]

4 Discussion

4.1 Interaction between β-secretase and APP fragment

Figure 1 displays the high capability of our wireless QCM biosensor for the long-time monitoring of the deposition reaction. BACE1 is recognized as a protease, and it cleaves APPs at the Aps site (Lichtenthaler *et al.* (1999)), creating the N-terminal of the Aβ peptides. This cleavage is facilitated by the Swedish mutation (Lys-Met/Asn-Leu mutation), and the APP fragment we used involves this mutation, for which we expect enhanced activity of BACE1.

10

Indeed, we succeeded in observing consecutive frequency decrease over 30 h from the channel on which the APP fragments were immobilized. This long deposition reaction is remarkable when compared with the hIgG-SPA binding reaction (standard specific interaction), which reaches the equilibrium state in much shorter time ($< \sim 1$ h). The total frequency decrement was nearly 20 kHz at 33 h. The frequency stability of the QCM biosensor used in the present study was about 30 Hz, and considering this value to be the detection limit, the detection of 20-kHz frequency decrement (three-orders of magnitude larger decrement) means significantly wide dynamic range of our QCM. Such a long monitoring has never been achieved with previous QCM studies. The experiment in Fig. 1 reveals that the cleaving reaction of the APP by β-secretase takes a long time, longer than 30 h.

4.2   Active nuclei formation by ultrasonication

Because Aβ peptides are cleaved from APPs in early endosomes at a lower pH (Rajendran *et al.* (2006)), it is important to study the monomer-adsorption capability of Aβ nuclei grown at a low pH. In the case of nucleus preparation by the agitation, the ThT level took the maximum value at pH 4.6 (Figure 2(c)). This is attributed to high solvent-exposure capability and low helix propensity of the central-hydrophobic-cluster (CHC) region at pH 4-6: There are two hydrophobic regions in the full-length Aβ peptide. One is near the C-terminal hydrophobic region (sequence 29-42), and the other is CHC between 17 and 21 (-Leu-Val-Phe-Phe-Ala-). Recent theoretical study reveals that the degree of solvent exposure of the C-terminal hydrophobic region is nearly independent of pH, but that of the CHC region is highly pH-dependent and becomes higher

11

at pH 4-6, while the helix propensity of the CHC region becomes lower at pH 4-6 (Khandogin and Brooks (2007)). Thus, the residual-structure change at the CHC region at pH4-6 can be the trigger for the transition from α helix to β-sheet, increasing the ThT level. Previous studies using bulk solutions also displayed high aggregation rates of Aβ peptides at pH 4-6 (Wood *et al.* (1996); Kirkitadze *et al.* (2001)). This modulation will be due to the intramolecular electrostatic interactions, and dimers and trimers are formed with the β-sheet-based structures. The nucleus observed using AFM showed spherical shape (not shown), and we consider that they are aggregates of the β-sheet-based oligomer.

The above interpretation for the pH-dependent aggregation behavior is, however, inapplicable to nuclei grown under ultrasonication, where the ThT level shows the maximum at pH 7.4 and remains fairly low level at pH 4.6 and 2.2 (Figure 2(c)). There are four possible effects cause by ultrasonication. First, the stirring effect, which could simply accelerate formation of nucleus by the agitation. However, this cannot be the principal factor in Figure 2(c) because of the different pH dependence between agitation and ultrasonication. (Simple acceleration of the aggregation reaction would have yielded the same pH dependence.) Second, local condensation of peptides due to cavitation bubbles created by ultrasound. The structure of aggregate will be dependent on the peptide concentration. Because cavitation bubbles are usually negatively charged (Takahashi (2005)), charged proteins collect on bubble surface, and they can be highly condensed after the bubble collapse. Ultrasonically generated cavitation bubbles repeat growth and collapse, and this condensation occurs every acoustic cycle. However, this is considered as a minor effect in the present case, since we expect positive charge of the peptide at pH 2.2 (lower

than the theoretical isoelectric point of 5.31), which would have enhanced the condensation to yield higher ThT level. Third, the structure change of peptide caused by the energy emission by the bubble collapse. The cavitation bubble collapse adiabatically in a very short time (~ 5 μs), which causes extremely high-temperature ($> \sim 1000$ °C) region near the bubble and induces thermally activated chemical reaction. Besides, free radial species are created near the bubble (Colussi *et al.* (1999)), which can make chemical reactions of high energy barriers proceed because of their high oxidization capability. Thus, high energy emission at the bubble collapse can cause chemical reactions which would never occur in standard conditions, and it may cause structural modulation of the Aβ peptide to form the β-sheet-based nuclei even at pH 7.4. And fourth, direct structural modulation for the peptide due to acoustic strain. When conformation-change rate to a specific structure matches with the ultrasonic strain period, the apparent energy barrier to the transition is reduced, and the structural modulation could occur. We suggest that third and fourth factors contribute to create high-ThT-level nucleus at neutral pH.

4.3   Heterogeneous deposition reaction and deposited structures

Frequency responses in Fig. 3 are not so smooth as those observed for other binding systems (in Fig. 1, for example). Unlike a usual antigen-antibody binding reaction with a single equilibrium constant, accumulation reaction of Aβ peptide progresses with much more complexity (Lomakin *et al.* (1996)). For example, in the case of attachment of an Aβ monomer on the fibril end, multiple kinetics should appear including the fibril-end kinetics for transition into the active end and the kinetics for monomer attachment, yielding the stop-and-

13

go growth of the fibril (Kellermayer *et al.* (2008)). In this case, we expect an uneven frequency response even in the macroscopic measurement, because all monomers are simultaneously dissolved to grow nuclei. Similar multi-kinetics mechanism could appear in the case of oligomer formation. Thus, we consider that the non-smooth frequency change is a characteristic in deposition reaction of the Aβ peptides.

It deserves attention that the dependence of deposition rate on the solution pH at which the nucleus was grown (Figure 4) apparently coincides with the pH dependence of the ThT fluorescence level of the nucleus (Figure 2(c)). This indicates that presence of β-sheet-related structure is essentially necessary for adsorbing monomer peptides. Remarkable observation is that the nucleus formed by ultrasonication at pH 7.4 yields considerably large deposition rate, which is larger than that on the agitation nucleus grown at pH 4.6 by a factor of 6. Because the maximum ThT level of the nucleus created by ultrasonication is nearly equal to that by the agitation (Figure 2(c)), we expect identical amounts of the β-sheet structure, indicating that ultrasonically produced nucleus possesses different structure from that formed by standard agitation processes, and it adsorbs Aβ monomer more effectively to form oligomeric deposits on the surface. Such a high deposition-rate model is practically important for development of drugs for disaggregation of the neurotoxic aggregates.

Finally, we emphasize that deposited structure with a high deposition rate is oligomeric without any observable fibrils (Figures 5(b) and 5(c)). This observation is severely different from aggregated structures observed in most previous works using bulk solutions, in which amyloid fibril structures dominates. This discrepancy may be caused by our characteristic deposition configuration,

14

where flowing monomer peptide interacts with immobilized nuclei on surface, excluding interaction among aggregations. This configuration is more closely related with AD in vivo and therefore will contribute to development of drugs for AD.

5 Conclusions

We established the long-time monitoring QCM system, and its capability was confirmed by the binding reaction of β-secretase with the immobilized APP fragment, showing monotonic frequency decrease over 30 h.

We have successfully performed long-time ($\sim$50 h) monitoring of the heterogeneous deposition reaction of $A\beta_{1-40}$ monomer on $A\beta_{1-42}$ nuclei grown by the agitation and ultrasonication at various pH. The deposition rate was highly pH dependent, and ultrasonication yielded the active nucleus, which significantly accelerates the deposition reaction compared with nuclei grown by the agitation. Because ThT levels of the nuclei are identical to each other, ultrasonication may cause different structural modulation in the peptide by reducing the apparent energy barrier for the structure transition, owing to high energy emission at the bubble collapse or frequency-matched strain field. The resultant deposition structures were oligomeric, which are considered to be more neurotoxic than fibrils, and this deposition model will play an important role in the drug development for AD.

Acknowledgement

References

Ban, T., Hoshino, M., Takahashi, S., Hamada, D., Hasegawa, K., Naiki, H., Goto, Y. J. Mol. Biol. 2004, 344, 757-767.

Benseny-Cases, N., Cocera, M., Cladera, J. Biochem. Biophys. Res. Commun. 2007, 361, 916-921.

Bitan, G., Kirkitadze, M. D., Lomakin, A., Vollers, S. S., Benedek, G. B., Teplow, D. B. Proc. Natl. Acad. Sci. USA. 2003, 100, 330-335.

Chatani, E., Lee, Y.-H., Yagi, H., Yoshimura, Y., Naiki, H., Goto, Y. Proc. Nat. Acad. Sci. USA. 2009, 106, 11119-11124.

Colussi, A. J., Hung, H.-M., Hoffmann, M. R. J. Phys. Chem. A. 1999, 103, 2696-2699.

Gravina, S. A., Ho, L. B., Eckman, C. B., Long, K. E., Otvos, L., Jr., Younkin, L. H., Suzuki, N., Younkin, S. G. J. Biol. Chem. 1995,270, 7013-7016.

Isaacs, A. M., Senn, D. B., Yuan, M., Shine, J. P., Yankner, B. A. J. Biol. Chem. 2006, 281, 27916-27923.

Iwatsubo, T., Odaka, A., Suzuki, N., Mizusawa, H., Nukina, N., Ihara, Y. Neuron 1994, 13, 45-53.

Jarrett, J. T., Berger, E. P., Lansbury, P. T., Jr. Biochemistry 1993, 32, 4693-4697.

Khandogin, J., Brooks III, C. L. Proc. Nat. Acad. Sci. USA. 2007, 104, 16880-16885.

Kirkitadze, M. D., Condron, M. M., Teplow, D. B. J. Mol. Biol. 2001, 312, 1103-1119.

Kellermayer, M. Z., Karsai, Á., Benke, M., Soós, K., Penke, B. Proc. Natl. Acad. Sci. USA 2008, 105, 141-144.

Klein, W. L., Krafft, G. A., Finch, C. E. Trends Neurosci. 2001, 24, 219-224.

17

Ladiwala, A. R. A., Lin, J. C., Bale, S. S., Marcelino-Cruz, A. M., Bhattacharya, M., Dordick, J. S., Tessier, P. M. J. Biol. Chem. 2010, 285, 24228-24237.

LaFerla, F. M., Green, K. N., Oddo, S. Nat. Rev. Neurosci. 2007, 8, 499-509.

Lambert, M. P., Barlow, A. K., Chromy, B. A., Edwards, C., Freed, R., Liosatos, M., Morgan, T. E., Rozovsky, I., Trommer, B., Viola,K. L., Wals, P., Zhang, C., Finch, C. E., Krafft, G. A., Klein, W. L. Proc. Natl. Acad. Sci. USA. 1998, 95, 6448-6453.

Lichtenthaler, S. F., Wang, R., Grimm, H., Uljon, S. N., Masters, C. L., Beyreuther, K. Proc. Natl Acad. Sci. USA. 1999. 96, 3053-3058.

Lomakin, A., Chung, D. S., Benedek, G. B., Kirschner, D. A., Teplow, D. B. Proc. Natl. Acad. Sci. USA 1996, 93, 1125-1129.

Mastrangelo, I. A., Ahmed, M., Sato, T., Liu, W., Wang, C., Hough, P., Smith, S. O. J. Mol. Biol. 2006, 358, 106-119.

Naiki, H., Higuchi, K., Hosokawa, M., Takeda, T. Anal. Biochem. 1989, 177, 244-249.

Naiki, H., Higuchi, K., Matsushima, K., Shimada, A., Chen, W. H., Hosokawa, M., Takeda, T. Lab. Invest. 1990, 62, 768-773.

Ogi, H., Hatanaka, K., Fukunishi, Y., Nagai, H., Hirao, M., Nishiyama, M. Jpn. J. Appl. Phys. 2009a, 48, 07GF01.

Ogi, H., Nagai, H., Fukunishi, Y., Hirao, M., Nishiyama, M. Anal. Chem. 2009b, 81, 8068-8073.

Ogi, H., Fukunishi, Y., Yanagida, T., Yagi, H., Goto, Y., Fukushima, M., Uesugi, K., Hirao, M. Anal. Chem. 2011, 83, 4982-4988.

Ohhashi, Y., Kihara, M., Naiki, H., Goto, Y. J. Biol. Chem. 2005, 280, 32843-32848.

O'Meara, G. M., Munro, P. A. Enzyme Microb. Technol. 1984, 280, 32843-

32848.

Rajendran, L.,Honsho, M., Zahn, T. R.,Keller, P.,Geiger, K. D.,Verkade, P.,Simons, K. Proc. Natl. Acad. Sci. USA. 2006, 103, 11172-11177.

Sauerbrey,G. Z.Phys. 1959, 155, 206-222.

So, M., Yagi, H., Sakurai, K., Ogi, H., Naiki, H., Goto, Y. J. Mol. Biol. 2011, 412, 568-577.

Suzuki, N., Cheung, T. T., Cai, X.-D., Odaka, A., Otvos, L., Jr., Eckman, C., Golde, T. E., Younkin, S. G. Science 1994, 264, 1336-1340.

Takahashi, M. J. Phys. Chem. B. 2005, 109, 21858-21864.

Wood, S. J., Maleeff, B., Hart, T., Wetzel, R. J. Mol. Biol. 1996, 256, 870-877.

Yan, R., Bienkowski, M. J., Shuck, M. E., Miao, H., Tory, M. C., Pauley, A. M., Brashler, J. R., Stratman, N. C., Mathews, W. R., Buhl, A. E., Carter, D. B., Tomasselli, A. G., Parodi, L. A., Heinrikson, R. L., Gurney, M. E. Nature 1999, 402, 533-537.

Figure Captions

Fig. 1 (Color online) Frequency changes during various binding reactions: 5 μg/ml BACE1 on APP fragment (Black), BSA (green), and glycine (blue); and 10 μg/ml hIgG on SPA (red). Note that a logarithmic time scale is used.

Fig. 2 (Color online) (a)Examples of evolutions of the ThT fluorescence level during growth of Aβ_{1-42} nuclei by the agitation and ultrasonication. (b)Change in the fluorescence spectrum during the agitation at pH 4.6. (c)Comparison of the ThT level of solutions prepared by the agitation for 48 h and by ultrasonication for 4 h.

Fig. 3 (Color online) Resonance frequency changes caused by the deposition of Aβ_{1-40} peptide on (a)nuclei grown by the agitation and (b)those by ultrasonication.

Fig. 4 (Color online) The deposition rate calculated from the frequency change at 50 h using the Sauerbrey equation.

Fig. 5 (Color online) AFM images (2.5 μm×2.5 μm) after the deposition reaction for 50 h on the sensor surfaces, on which various nuclei were immobilized: (a)agitation nucleus grown for 48 h at pH 7.4, (b)that at pH 4.6, (c)ultrasonicated nucleus grown for 4 h at pH 7.4, and (d) that at pH 4.6.
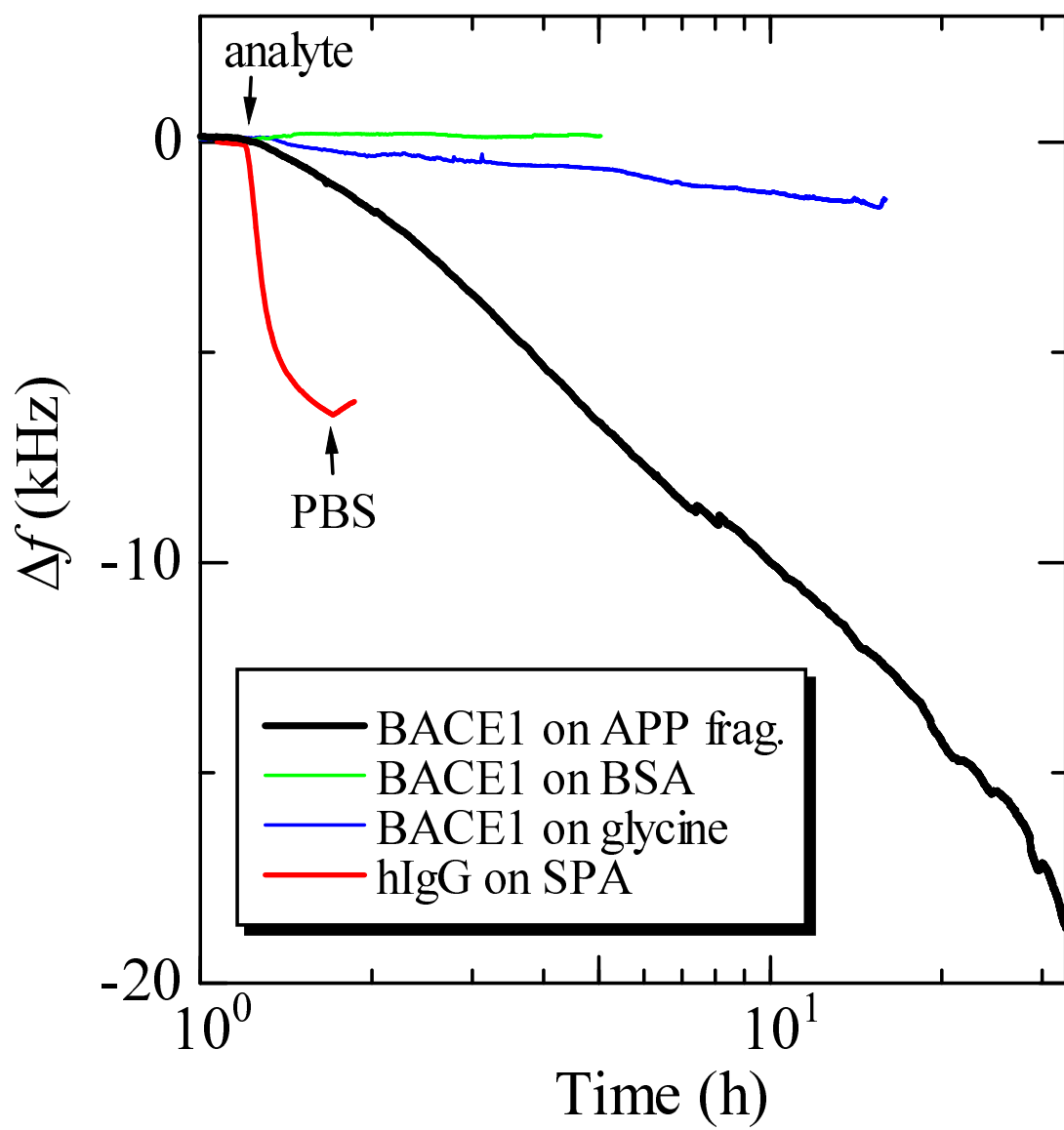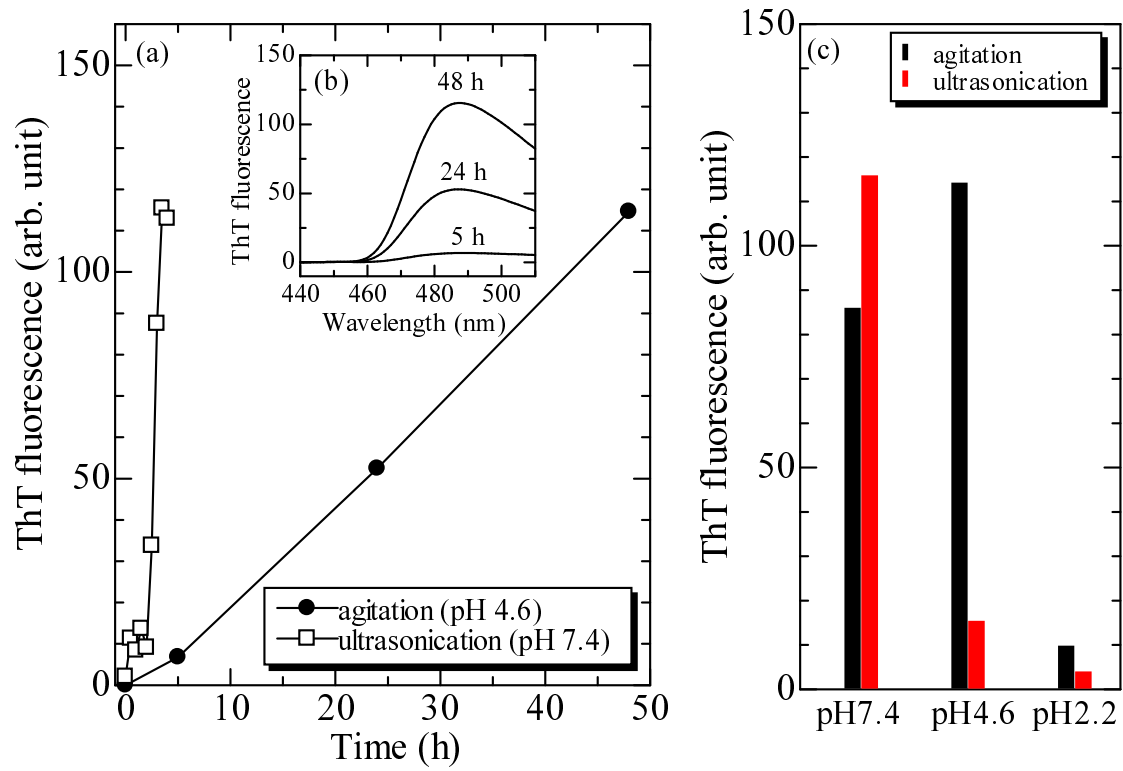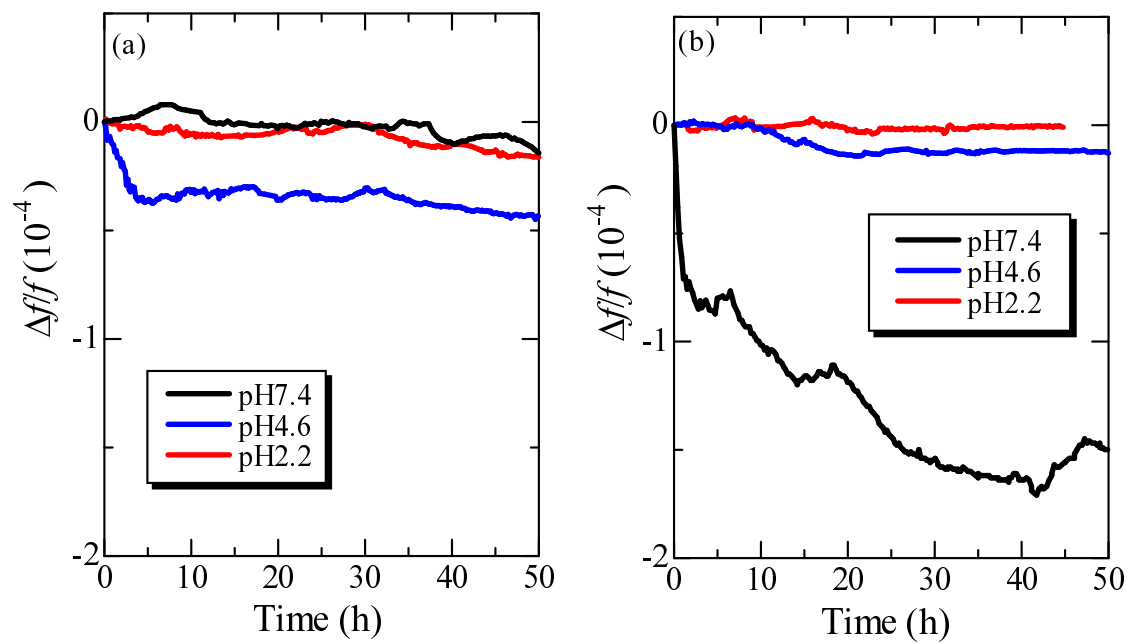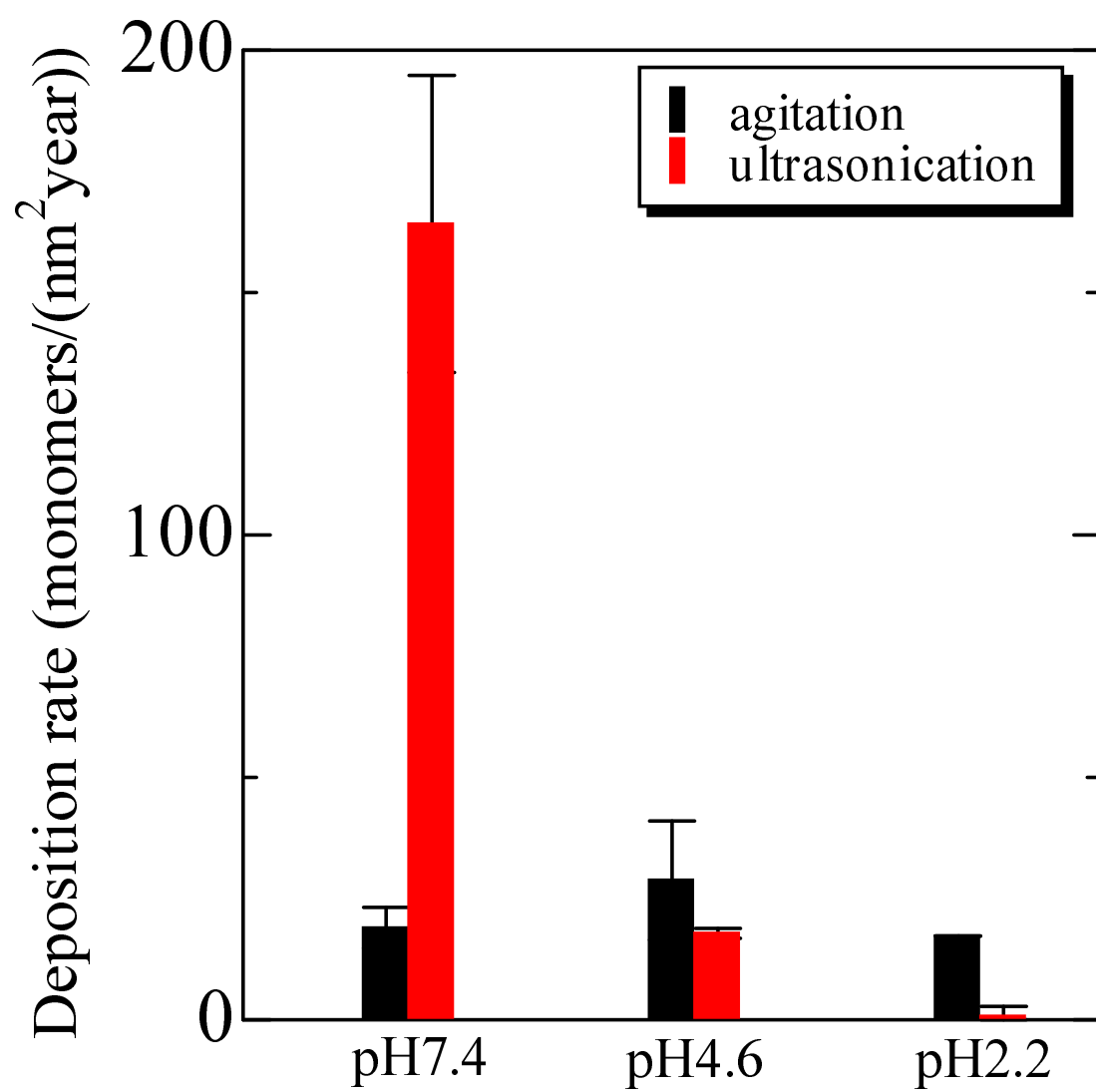
Fig. 1.

Fig. 2.

Fig. 3.

Fig. 4.

Fig. 5.